ACADEMIC PRESS

Available online at www.sciencedirect.com
SCIENCE DIRECT®

Journal of Catalysis 213 (2003) 296–304

JOURNAL OF CATALYSIS

www.elsevier.com/locate/jcat

Flame-made platinum/alumina: structural properties and catalytic behaviour in enantioselective hydrogenation

Reto Strobel,[a,b] Wendelin J. Stark,[a,b] Lutz Mädler,[b] Sotiris E. Pratsinis,[b] and Alfons Baiker[a,*]

[a] *Laboratory of Technical Chemistry, ETH Hönggerberg, CH-8093 Zurich, Switzerland*
[b] *Particle Technology Laboratory, Department of Mechanical and Process Engineering, ETH Zentrum, CH-8092 Zurich, Switzerland*

Received 18 July 2002; revised 26 August 2002; accepted 20 September 2002

Abstract

Flame spray pyrolysis (FSP) has been used for the production of alumina-supported platinum catalysts (1 to 10 wt% Pt on alumina). Liquid precursors containing specific amounts of aluminium isopropoxide and platinum acetylacetonate dissolved in xylene/ethylacetate were dispersed by oxygen and combusted, resulting in nanostructured powders. The as-prepared powders were collected on a filter and characterised by high-resolution transmission electron microscopy, hydrogen chemisorption, nitrogen adsorption, X-ray diffraction, and laser ablation inductively coupled plasma mass spectrometry. The specific surface areas of the powders ranged from 70 to 140 m^2/g depending on the oxygen and precursor flow rates. Platinum was well dispersed and confined to the alumina surface. Platinum dispersion strongly depended on the platinum loading, decreasing from ca. 77 to 24% when the loading was increased from 0.1 to 0.9 $mg_{Pt}\,m^{-2}$. These FSP-made catalysts showed higher activity for the enantioselective hydrogenation of ethyl pyruvate than a standard commercial platinum/alumina catalyst (E4759) with about the same platinum loading. Enantiomeric excess of (*R*)-ethyl lactate formation reached 87% at 100% conversion for FSP-derived catalysts pretreated in hydrogen. Turnover frequency increased with higher platinum loading, i.e., lower dispersion, indicating structure sensitivity of the reaction. In contrast, enantiomeric excess was virtually independent of platinum loading in the range 0.2–0.9 $mg_{Pt}\,m^{-2}$.

Keywords: Flame spray pyrolysis; Platinum; Alumina; Chiral; Asymmetric; Enantioselective; Hydrogenation; Ethyl pyruvate

1. Introduction

Supported platinum catalysts are widely used in many chemical processes, such as hydrogenation, oxidation, and reforming. Much effort has been devoted to the development of platinum-based catalytic materials [1]. Flame synthesis is a relatively new method for the one-step production of supported metal catalysts [2,3]. Flame aerosol synthesis has been shown to produce highly active catalysts for the selective reduction of NO by NH_3 [4] and the selective epoxidation of olefins [5]. Choy and Seh [6] reported the production of Ni/Al_2O_3 reforming catalysts by flame-assisted vapor deposition. Moser et al. [2] showed the flame aerosol synthesis of noble metals supported on Al_2O_3 with very low specific surface areas (10 $m^2\,g^{-1}$). Very recently Johannessen and Koutsopoulos [3] prepared Pt/TiO_2 catalysts for SO_2 oxidation using an aerosol flame reactor. Since the platinum precursor shows very low volatility they operated at very low production rates (on the order of mg/h).

In general, flame synthesis is a fast, cost-effective, and versatile process for the production of ceramic nanoparticles [7,8]. In this process, a flame is used to drive chemical reactions of precursor compounds, resulting in the formation of clusters, which grow to nanometer-sized products by coagulation and sintering. Flame spray pyrolysis (FSP) has been used for the synthesis of alumina powders [9]. Ulrich [10] suggested the use of flame-made materials for catalytic applications in 1984, but to our best knowledge, no research was undertaken yet to test the catalytic potential of flame-made platinum/alumina nanoparticles for hydrogenation.

Since its discovery by Orito and co-workers [11–14], several groups have investigated the platinum–cinchona system for the enantioselective hydrogenation of α-ketoesters. Considerable knowledge has been built up concerning reaction parameters and functioning of this complex catalytic system [15–19]. At present, the most widely used catalyst for

* Corresponding author.
E-mail address: baiker@tech.chem.ethz.ch (A. Baiker).

0021-9517/02/$ – see front matter
doi:10.1016/S0021-9517(02)00082-9

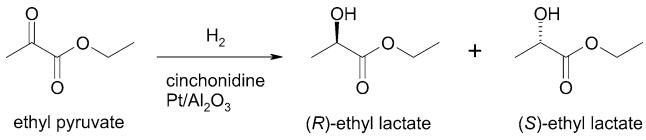

Scheme 1.

the enantioselective hydrogenation of ethyl pyruvate in the presence of cinchonidine (Scheme 1) is 5 wt% Pt/Al_2O_3 with relatively low dispersion and rather large pore volume [20]. Other support materials are also suitable, such as TiO_2, SiO_2, carbon, clays, and zeolites [20–22]. The enantioselective hydrogenation of ethyl pyruvate is used here as a test reaction to explore the catalytic behaviour of Pt/Al_2O_3 made by flame spray pyrolysis. Structural and catalytic properties of this material will be compared to those of a standard commercial Pt/Al_2O_3 catalyst for this reaction.

2. Experimental

2.1. Catalyst preparation

Figure 1 illustrates the experimental setup for the synthesis of Pt/Al_2O_3 by flame spray pyrolysis [23,24]. Precursor solutions were prepared by dissolving appropriate amounts of aluminium isopropoxide ($Al(i\text{-}PrO)_3$, Fluka, 97%) and platinum acetylacetonate ($Pt(acac)_2$, Strem, 98%) in xylene (Riedel deHaen, 96%)/ethylacetate (Fluka, 99.5%) mixtures (65 : 35 vol/vol). The aluminium concentration was always 0.67 M. Precursor solutions were stored at 50 °C to prevent precursor precipitation. In a typical run, the liquid precursor mixture was fed into the center of a methane/oxygen flame by a syringe pump (Inotech R232) and dispersed by oxygen (Pan Gas, > 99.95%), forming a fine spray. The pressure drop at the capillary tip (1.5 bar) was kept constant by adjusting the orifice gap area at the nozzle. The spray flame was surrounded and ignited by a smaller flame ring issuing from an annular gap (0.15 mm spacing, at a radius of 6 mm). This premixed methane/oxygen supporting flame was kept constant for all experiments at a total flow rate of 4.7 L/min with fuel/oxygen ratio $\phi = 0.92$ [25]. A sintered metal plate ring (8 mm wide, starting at a radius of 8 mm) provided an additional oxygen sheath flow (5 L/min) surrounding the supporting flame. Calibrated mass flow controllers (Bronkhorst) were used to monitor all gas flows. Product particles were collected on a glass fibre filter (Whatmann GF/A, 15 cm in diameter) with the aid of a vacuum pump (Vaccubrand). The liquid feed rate (3–6 ml/min) and the oxygen flow rate (2–6 L/min) were varied during experiments. The resulting materials are designated as $x\text{Pt}y/z$, where x denotes the weight fraction of platinum, y the liquid feed rate in ml/min, and z the oxygen flow rate in L/min. A standard commercial platinum/alumina catalyst (Engelhard, E4759) was used as a reference material. Properties of this catalyst are listed in Table 1.

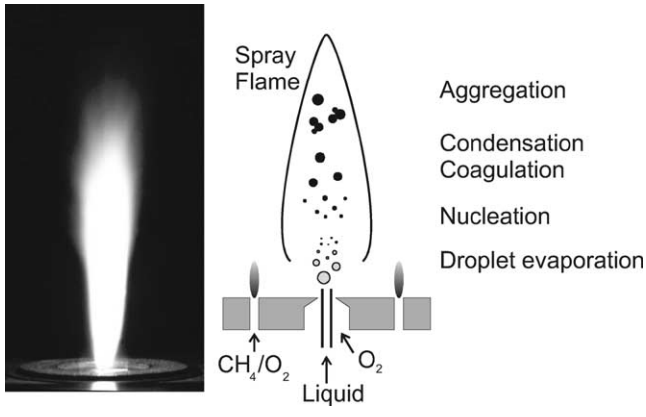

Fig. 1. Sketch of a typical flame spray pyrolysis unit. The precursor mixture is rapidly dispersed by oxygen and fed into the premixed methane/oxygen stream. After evaporation and burning of the precursor, particles are formed by condensation, coalescence and coagulation. The photograph shows a typical spray flame producing alumina nanoparticles.

2.2. Catalyst characterisation

The specific surface area (SSA) of the as-prepared samples was determined by nitrogen adsorption at 77 K using the BET method (Micromeritics GEMINI 2360). All samples were outgassed at 150 °C for 1 h. The results were cross-checked by recording a full adsorption isotherm of the as-prepared powder (Micromeritics ASAP 2010 Multigas system). To determine the pore size distribution the desorption isotherm was used.

The powder X-ray diffraction spectra were recorded with a Bruker D8 advance diffractometer from 20° to 70°, step size 0.02°, at a scan speed of 0.24 °/min.

Laser ablation inductively coupled plasma mass spectrometry (LA-ICP-MS) was used to determine the elemental composition of a representative catalyst. A 193-nm Excimer laser system (GeoLas, MicroLas, Göttingen, Germany) coupled to a ICP-MS (ELAN 6100, Perkin–Elmer, Norwalk, MA), extensively described in [26], has been used in standard mode to determine the Pt concentration. The samples were ablated under helium atmosphere using a 60-µm crater diameter at a repetition rate of 10 Hz. External calibration was carried out using Reference 610 from NIST and the Al signal was used as an internal standard quantification.

The high-resolution transmission electron microscopy (HRTEM) investigations were performed with a CM30ST microscope (Philips: LaB6 cathode, operated at 300 kV, point resolution ∼ 2 Å). Particles were deposited onto a carbon foil supported on a copper grid. The Pt particle size distribution was derived from TEM images, using the software Optimas (Version 6.5). The surface average and the number average particle diameter were calculated according to

$$\langle d_A \rangle = \frac{\sum N_i d_i^3}{\sum N_i d_i^2} \quad \text{and} \quad \langle d_N \rangle = \frac{\sum N_i d_i}{\sum N_i}.$$

Table 1
Textural properties and catalytic behaviour of platinum/alumina prepared by FSP in the enantioselective hydrogenation of ethyl pyruvate

Sample	Pt content/wt%	BET[a] $/m^2\,g^{-1}$	Pretreat.[b]	Pt disp./%	TOF[c] $/s^{-1}$	r_0[d] $/mol\,kg_{Pt}^{-1}\,s^{-1}$	*ee*/%
0Pt3/3	0	116	no	–	0	0	–
1Pt3/3	1	109	no	77	0.2	0.9	75 ± 5[e]
1Pt3/3	1	109	yes	–	4.8	**19.3**	79
2Pt3/3	2	107	no	40	1.6	3.3	75
5Pt3/3	5 (5.63)[f]	112	no	32	3.1	5.3	75
5Pt3/3	5	112	yes	–	5.5	**8.9**	**87**
5Pt3/3s[g]	5	112	no	8	4.6	2.0	73
5Pt3/3s[g]	5	112	yes	–	9.6	4.0	80
5Pt5/3	5	87	no	30	3.8	5.8	75
7.5Pt3/3	7.5	112	no	27	4.5	6.3	76
10Pt3/3	10	110	no	24	3.6	4.5	75
E4759	5	95	no	22	3.2	3.7	83
E4759	5	–	yes		3.7	**4.2**	**92**

Except for sample 5Pt5/3 all catalysts were prepared with the same flame conditions. The commercial catalyst E4759 is quoted as a reference.
[a] Reproducibility error ± 3%.
[b] H_2 400 °C, 90 min.
[c] TOF is given per surface atoms, determined by H_2 chemisorption.
[d] Determined from initial hydrogen uptake.
[e] Due to low conversion *ee* could not be determined with the same accuracy as for the other samples ± 0.5%.
[f] Nominal content (measured by LA-ICP-MS).
[g] Sintered (air, 600 °C, 2 h).

The geometric standard deviations of the number ($\sigma_{g,N}$)- and the volume ($\sigma_{g,V}$)-based particle size distribution were calculated according to

$$\ln \sigma_{g,x} = \left(\frac{\sum N_i (\ln d_i - \ln\langle d_x \rangle)^2}{N_{\text{total}} - 1} \right)^{1/2},$$

with x being N or V, respectively.

The platinum dispersion was determined using H_2 chemisorption on samples freshly reduced at 350 °C for 2 h under flowing hydrogen and evacuated at the same temperature. Varying the pretreatment temperature between 250 and 400 °C did not affect the degree of dispersion. Platinum started sintering at temperatures above 400 °C as indicated by a drop in dispersion. The H_2 chemisorption analysis was carried out at 35 °C using the double isotherm method [27] (Micromeritics ASAP 2010 Multigas system). The degree of dispersion was calculated from the amount of chemisorbed H_2 assuming a stoichiometric factor (H/Pt) of 1 [28].

2.3. Catalytic studies

The hydrogenation reactions were carried out batchwise using a catalytic screening unit (Argonaut Endeavour) equipped with eight autoclaves. In order to assess standard conditions, a series of experiments were performed. To rule out mass transfer limitations the influence of H_2 pressure, stirring revolution, and amount of catalyst was evaluated [29]. Standard reactions were performed at room temperature, 20 bar H_2 pressure, and 750 rpm stirring revolution. The reaction mixtures consisted of 10 mg catalyst, 0.4 ml ethyl pyruvate (Fluka, > 97%, freshly distilled prior to use), 0.5 mg cinchonidine (Fluka, > 98%) as modifier, and 4.6 ml acetic acid (Fluka, > 99.8%) as solvent, resulting in a total reaction volume of 5 ml. The reaction was initiated by starting the mechanical stirring. Initial reaction rates were calculated from monitored hydrogen consumption. After the reaction was stopped, samples of the mixtures were taken, filtrated, and analysed using an HP 6890 gas chromatograph equipped with a capillary column (Chirasil-DEX CB). The enantiomeric excess (*ee*) was calculated according to $ee(\%) = |R(\%) - S(\%)|$.

Some catalysts were tested in a glass reactor equipped with two septa, one serving as H_2 inlet and the other for withdrawing samples. Conditions were the same as mentioned above, but hydrogen pressure was 1 bar. Conversion and enantioselectivity were followed by taking samples of the reaction mixture after defined time intervals and subsequent gas chromatographic analysis. In some experiments the catalysts were subjected to a reductive pretreatment before the hydrogenation was started. This catalyst prereduction was performed in a U-tube at 400 °C under flowing hydrogen for 90 min.

3. Results

3.1. Catalyst properties

Flame spray pyrolysis (FSP) of the platinum/alumina precursor solution resulted in spherical alumina particles in the size range of 10 to 30 nm with well-dispersed Pt-metal particles. Two series of Pt/Al_2O_3 catalysts were prepared by changing the amount of platinum (0–10 wt%) using the same flame conditions (liquid feed rate: 3 ml/min; O_2 flow rate: 3 L/min) and with 5 wt% platinum under different flame

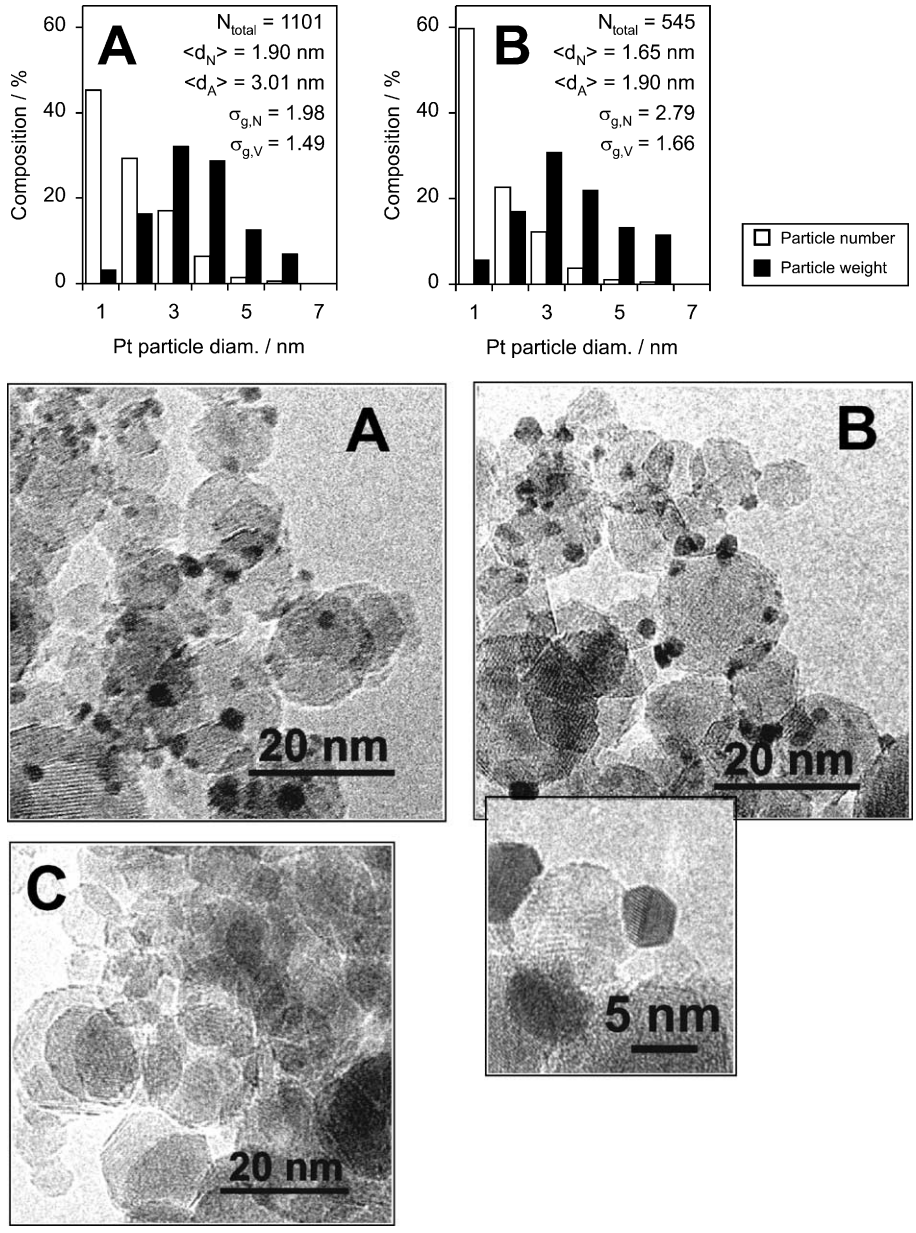

Fig. 2. Transmission electron micrographs of flame-made Pt/Al_2O_3 particles. Platinum/alumina prepared at 3 ml/min precursor flow and 3 L/min O_2 containing (A) 10 (10Pt3/3), (B) 5 (5Pt3/3), and (C) 1 wt% Pt (1Pt3/3). The corresponding Pt particle size distributions of N_{total} measured particles with geometric standard deviation ($\sigma_{g,N}$, $\sigma_{g,V}$) and average diameters ($\langle d_N \rangle$, $\langle d_A \rangle$) obtained from the TEM micrograph are given at the top. The inset in (B) shows a magnification of the edged shaped Pt particles with lattice planes.

conditions (liquid feed rate: 2–6 ml/min; O_2 flow rate: 3–6 L/min).

Table 1 gives an overview of structural and catalytic data measured for FSP-derived materials and a standard commercial Pt/Al_2O_3 catalyst used as a reference. LA-ICP-MS measurements confirmed that no platinum was lost in the preparation procedure, affording closely the nominal platinum content (5.6 wt% Pt for 5Pt3/3).

Figure 2 shows HRTEM images of the FSP derived Pt/Al_2O_3 catalysts with different Pt contents prepared under identical flame conditions (liquid feed rate 3 ml/min, O_2 flow rate 3 L/min). The platinum particles, with a diameter of 1 to 6 nm, are confined to the surface of the alumina particles. Crystalline areas of γ-Al_2O_3 are visible in all samples. Platinum particle size distributions derived from HRTEM images show smaller particles for lower Pt content (Fig. 2). At 1 wt% platinum content it was not possible to determine the particle size distribution, because of the lack of HRTEM resolution. A close view of a single Pt particle reveals pronounced edges (inset B). Figure 3 depicts a HRTEM image of the reference catalyst E4759. The material consists of γ-Al_2O_3 and deposited platinum particles with

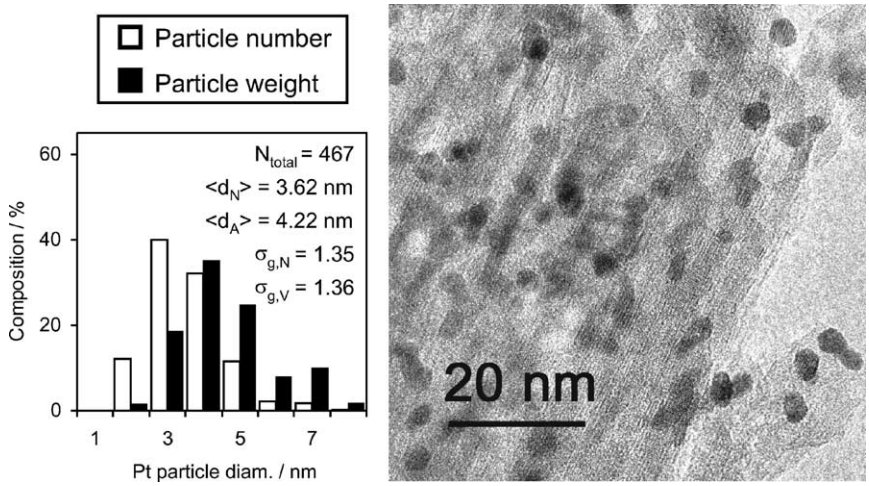

Fig. 3. Transmission electron micrograph of commercial reference catalyst (E4759). The Pt particle size distribution of N_{total} measured particles, geometric standard deviation ($\sigma_{g,N}$, $\sigma_{g,V}$) and average diameter ($\langle d_N \rangle$, $\langle d_A \rangle$) are given on the left-hand side.

diameters from 2 to 8 nm. Metal particle size distribution derived from the TEM image shows larger platinum particles than the FSP-derived catalysts (Fig. 2).

To investigate the influence of the preparation conditions on the material properties and their catalytic activity, samples were prepared at different oxygen gas flow rates and changing production rates. Figure 4 shows the BET specific surface area of powders prepared with different production rates (corresponding to liquid feed rates of 3–6 ml/min) at 3 L/min oxygen flow and at a constant ratio between production rates and oxygen flow (1 L/ml, O_2/liquid feed). At a constant oxygen flow rate (3 L/min) higher production rates lead to lower specific surface areas (79 m^2/g for 5Pt6/3), while low production rates afford surface areas up to 140 m^2/g (5Pt2/3). If the production rate and the oxygen flow are increased at the same time (keeping the gas-to-liquid ratios constant), the specific surface area stays almost constant (Fig. 4). The platinum loading (up to 10 wt%) had no significant influence on the specific surface area when the same flame conditions are used (Table 1).

Figure 5 depicts the adsorption isotherms and the pore size distributions of a typical flame-made powder (5Pt3/3) and the E4759 catalyst as determined by the desorption branch of a full isotherm. Both materials possess similar

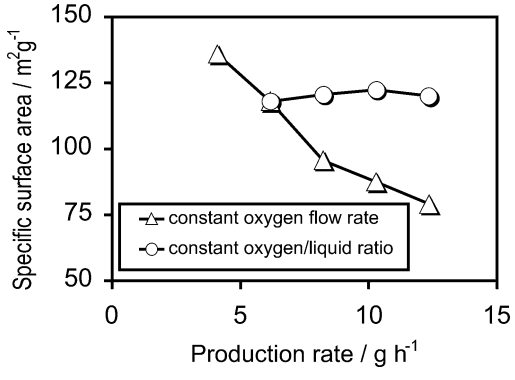

Fig. 4. Specific surface area of 5 wt% Pt/Al_2O_3 samples (5Ptx/y) as a function of production rate (corresponding to increasing the FSP liquid feed rate from 3 to 6 ml/min). When the oxygen flow rate is kept constant at 3 L/min the specific surface area decreases with higher production rate. The specific surface area is not significantly affected if the ratio between oxygen flow rate and production rate is kept constant (1 L/ml, O_2/liquid feed), while the production rate increases from 4 to 13 g/h.

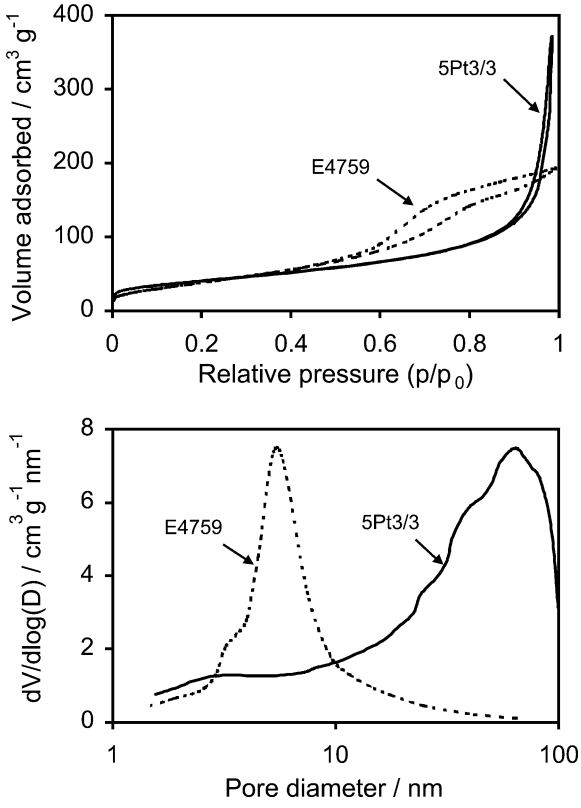

Fig. 5. Nitrogen adsorption isotherms and corresponding pore size distributions of a typical FSP-derived powder (5Pt3/3) and the commercial reference catalyst E4759. Note that the particles of the flame-made catalyst are virtually nonporous. The indicated macropores originate from interstitial voids of the agglomerated particles.

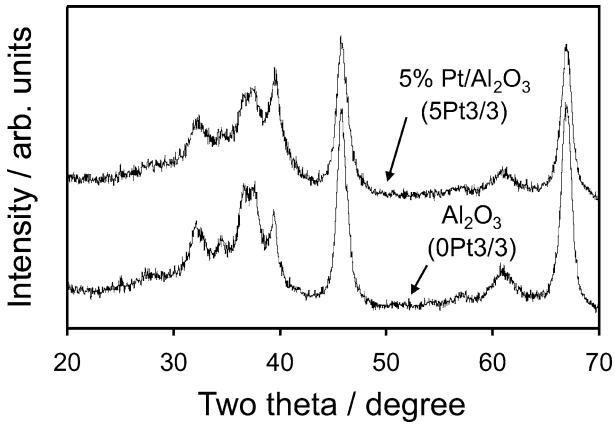

Fig. 6. XRD pattern of Al_2O_3 and 5 wt% Pt/Al_2O_3 indicating γ-alumina. The presence of platinum in the flame had no significant influence on the alumina crystal phase formation.

specific surface areas. However, the flame-made powder does contain virtually only macropores which originate from particles agglomeration, whereas the commercial standard catalyst E4759 is a mesoporous material. The influence on the alumina crystal phase in presence of platinum in the flame was investigated by X-ray diffraction. Figure 6 shows the Pt/Al_2O_3 XRD patterns for samples containing 0 and 5 wt% Pt (0Pt3/3 and 5Pt3/3) with slightly amorphous γ-Al_2O_3. The addition of Pt had no detectable influence on the alumina phase composition.

Figure 7 shows the platinum dispersion determined by H_2 chemisorption measurements as a function of the metal loading that was calculated from the nominal Pt content divided by the specific surface area. Low platinum loading leads to high platinum dispersion (up to 77% for the 1Pt3/3 catalyst). Higher metal loading than ca. 0.1 $mg_{Pt}\,m^{-2}$ results in a strong decrease of platinum dispersion. Figure 8 depicts the influence of the hydrogen pretreatment temperature on the platinum dispersion. Metal dispersion remains stable up to temperatures of 400 °C. Above that platinum starts sintering, followed by a drop in dispersion. Sintering of catalysts in air at 600 °C for 2 h caused the formation

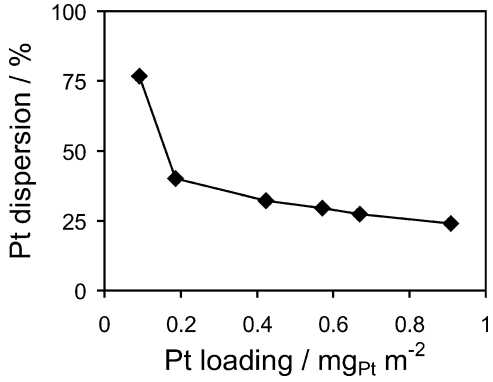

Fig. 7. Platinum dispersion determined from H_2 chemisorption measurements as a function of Pt loading. Dispersion ranges from 24% for the 10Pt3/3 up to 77% for the 1Pt3/3 sample.

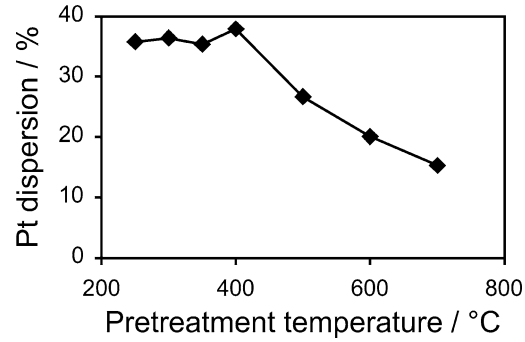

Fig. 8. Platinum dispersion of a typical sample (5Pt3/3) as a function of H_2 pretreatment. Platinum starts sintering above 400 °C indicated by a drop of dispersion.

of larger platinum particles, reducing the surface area for H_2 chemisorption (e.g., for 5Pt3/3 from 32 to 8% after sintering) and resulting in lower activity (Fig. 10).

3.2. Enantioselective hydrogenation

As-prepared materials were tested for the enantioselective hydrogenation of ethyl pyruvate. Figure 9 compares conversion and enantioselectivity at 1 bar H_2 pressure for a typical FSP-derived Pt/Al_2O_3 (5Pt3/3) with those of the commercial standard catalyst E4759 (5 wt% Pt on γ-alumina) used for this reaction. Both catalysts reach enantiomeric excess (*ee*) of about 70% at 100% conversion. However, the hydrogenation with the flame-made material is significantly faster.

Further catalytic measurements were carried out at 20 bar H_2 pressure and all enantiomeric excesses refer to 100% conversion. Figure 10 shows the dependence of the activ-

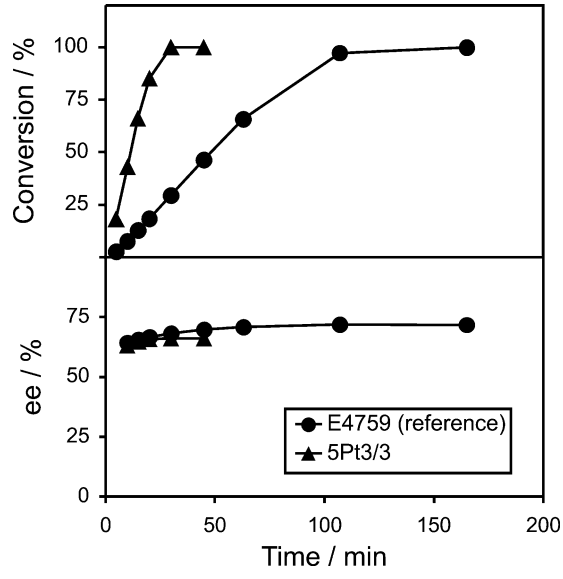

Fig. 9. Conversion and enantiomeric excess (*ee*) for the asymmetric hydrogenation of ethyl pyruvate at 1 bar H_2 pressure as a function of reaction time. The flame-made catalyst shows higher activity than the commercial reference catalyst (E4759).

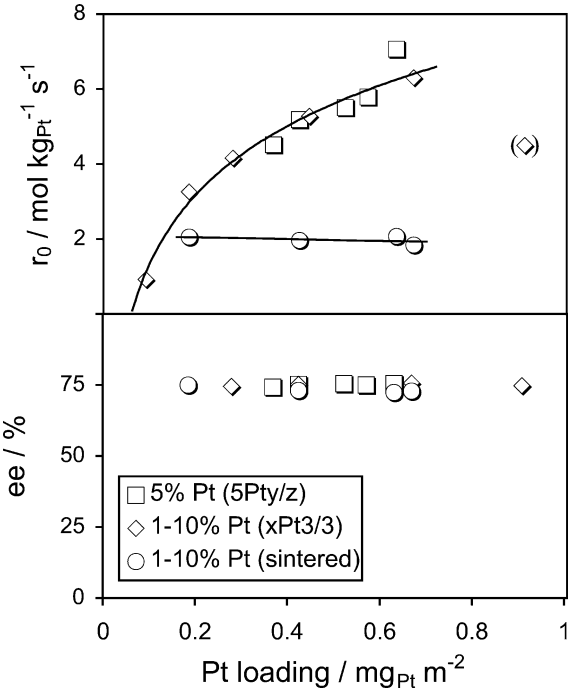

Fig. 10. Enantiomeric excess in the formation of (*R*)-ethyl lactate and initial hydrogen consumption rate as a function of Pt loading on the Al_2O_3-surface. While enantioselectivity remains virtually unaffected, the TOF increases with higher specific metal loading on the surface. For the catalyst with the highest loading (diamond) (10Pt3/3) hydrogen mass transfer strongly limited the reaction rate. Sintered samples (600 °C, air, 2 h) show the same enantioselectivity, but lower activity independent of metal loading.

ity and the enantioselectivity on the Pt loading of different flame-made catalysts. The enantiomeric excess stays constant at around 75% for all samples, independent of platinum content (1 to 10 wt%) and specific surface area resulting from different flame conditions (liquid flow: 2–6 ml/min, oxygen flow: 3–6 L/min) during preparation (Fig. 4). Initial reaction rates per platinum increase with higher platinum loading on the surface, but they are not affected by changing flame conditions. Sintered samples (air, 600 °C, 2 h) with different metal loading show all the same activity. Figure 11 gives the turnover frequencies of hydrogenation for various flame-made catalysts with different Pt dispersion. It shows clearly that turnover frequency strongly depends on Pt-dispersion; i.e., platinum atoms in larger particles possesses higher intrinsic activity.

Table 1 gives an overview of catalytic data for different FSP-made catalysts and the standard Pt/Al_2O_3 catalyst. A pure alumina sample (0Pt3/3) showed no activity in the hydrogenation of ethyl pyruvate. Decreasing the platinum dispersion led to higher reaction rates per platinum, i.e., higher turnover frequencies, whereas the enantioselectivity seemed not to be significantly affected by the metal dispersion in the range investigated. Samples were tested either as prepared or after pretreatment under hydrogen at 400 °C. The hydrogen pretreatment of the catalyst increased the enantioselectivity to (*R*)-ethyl lactate formation

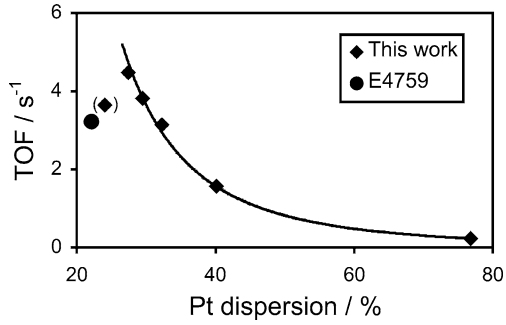

Fig. 11. Turnover frequency as a function of platinum dispersion for different flame-made materials and the reference catalyst (E4759). Materials consisting of larger Pt particles lead to more active catalysts. For the catalyst with the lowest dispersion (diamond) (10Pt3/3) hydrogen mass transfer strongly limited the reaction rate.

for all flame-made powders (from 75 up to 87% *ee*) and for the reference catalyst (from 82 to 92% *ee*). Interestingly, reaction rates increased strongly for flame-made powders (from 5.3 to 8.9 $mol\,kg_{Pt}^{-1}\,s^{-1}$ for 5Pt3/3, and from 0.9 to 19.3 $mol\,kg_{Pt}^{-1}\,s^{-1}$ for 1Pt3/3), while the reaction rate of the reference E4759 catalyst was comparatively little improved (from 3.7 to 4.2 $mol\,kg_{Pt}^{-1}\,s^{-1}$) by the pretreatment.

4. Discussion

4.1. Catalyst properties

The alumina constituent of the Pt/Al_2O_3 made by flame spray pyrolysis consists mainly of spherical γ-alumina particles. Other authors [7,30], using a flame synthesis process, have already reported this morphology. Adding platinum does not affect significantly the morphology of the alumina support. The size of the alumina particles, however, strongly depends on the synthesis conditions. Increasing the powder production rate while keeping the oxygen flow rate constant leads to larger flames and prolonged particle residence times at high temperature. Therefore larger particles are formed by coalescence and sintering [24,31]. The specific surface area was varied here from 70 to 140 $m^2\,g^{-1}$ by changing the production rate. In comparison, alumina made by wet-phase processes forms materials with specific surface areas up to about 600 $m^2\,g^{-1}$ [32,33]. Keeping the ratio between precursor feed and oxygen flow constant, thus increasing the production rate (6–13 $g\,h^{-1}$), results in similar flames and does not affect the specific surface area (Fig. 4). This is generally the case for flame spray pyrolysis of oxides and has already been reported for CeO_2 [24].

Platinum forms facetted particles on the alumina surface ranging from 1 to 6 nm in diameter (Fig. 2), which is consistent with the literature [3]. In general, higher platinum loadings lead to larger particles (Fig. 2) and consequently lower metal dispersions (Fig. 7). The platinum dispersion is only affected by the platinum loading itself, whereas flame conditions seem to have no significant effect within the parameter range investigated (Fig. 7).

Alumina has a very low vapor pressure and precipitates extremely fast in the hot environment of the flame. Platinum can form different oxides depending on temperature and gas composition. At low temperatures, platinum metal is the preferred form, even in an oxidative atmosphere [34]. It may be assumed that at least some PtO_x is formed in the flame. Platinum is known to be relatively volatile at elevated temperatures [34]. Since Pt/PtO_x is volatile at the temperatures reached in the flame (above 2000 °C), it remains in the vapor phase during alumina particle formation. Further downstream in the flame Pt/PtO_x starts to form small particles and/or deposits directly on the alumina surface. These Pt/PtO_x primary particles further grow mainly by sintering. It may be assumed that Pt/PtO_x is quite mobile on the alumina surface at the temperatures reached in the flame. Platinum has been reported to sinter above 500 °C, indicating good mobility [35,36]. In the flame process, residence times are very short and may prohibit the formation of larger particles. Johannessen and Koutsopoulos proposed a similar mechanism for the formation of Pt/TiO_2 in a flame synthesis process [3]. Further investigations on platinum particle formation are necessary to elucidate the mechanism of particle formation and deposition.

4.2. Enantioselective hydrogenation

The flame-made Pt/Al_2O_3 materials are very suitable catalysts for the enantioselective hydrogenation of ethyl pyruvate, in terms of both activity and enantioselectivity. They show slightly lower enantioselectivity but much improved activity, compared to the commonly used commercial E4759 catalyst (Table 1) [20,37]. Interestingly, the degree of platinum dispersion (from 24 to 77%) has no marked effect on the enantioselectivity of the reaction (Figs. 7 and 10). In earlier studies on platinum/alumina catalysts prepared by wet-chemical routes [20,37], Pt dispersion was reported to have a significant influence on the enantioselectivity. Specifically, catalysts with high dispersions corresponding to a mean platinum particle size lower than about 3 nm were found to exhibit lower enantioselectivity. Several factors may explain this behaviour. First of all, in the micromesoporous alumina-supported catalysts used in the previous investigations the small platinum particles may have been deposited in relatively narrow pores, which are not accessible for the bulky cinchonidine used as chiral modifier. Furthermore, in these studies the degree of dispersion was changed by different pretreatment conditions. Such pretreatments may affect not only the dispersion but also the morphological and chemical properties of the platinum particles [38,39]. Several studies [40,41] indicate that the shape of the metal particles may also play an important role to achieve high enantiomeric excesses. Especially, faceted platinum particles seem favourable compared to spherically shaped particles. The nonporous flame-made powders contain mainly faceted metal particles (Fig. 2) and exhibit good selectivities for the hydrogenation of ethyl pyruvate.

Interestingly, the activity expressed as turnover frequency depends strongly on the metal dispersion. Catalysts with higher platinum dispersion (above 40%) show significantly lower turnover frequencies (Fig. 11). Lower activity of the highly dispersed platinum has also been observed with conventionally prepared catalysts [16,42]. The higher activity of the FSP-derived materials compared to the commercial catalyst may be attributed to the higher accessibility of the platinum on the FSP-made material [20]. The structure of flame-made nanoparticles is very open and large aggregates give rise to some macroporosity (Fig. 5). This facilitates reactant and modifier diffusion and provides optimal conditions for mass transfer. Hydrogen pretreatment at elevated temperatures improves the enantioselectivity for all tested catalysts, probably due to structural rearrangement of the platinum surface atoms [41,43]. The strongest increase in activity (from 0.9 to 19.7 $\mathrm{mol\,kg_{Pt}^{-1}\,s^{-1}}$ for catalyst 1Pt3/3) was found for flame-made materials. Finally, the fact that neither the specific surface areas nor the catalytic properties of flame-made materials are affected by increasing the production rate and the oxygen flow is a promising feature for possible scaling-up of this catalyst production.

5. Conclusions

The flame spray pyrolysis method has been successfully applied for synthesis of Pt/Al_2O_3 hydrogenation catalysts. Materials with good catalytic performance in the asymmetric hydrogenation of ethyl pyruvate can be produced in a one-step flame synthesis process. The alumina support is made of agglomerated, nonporous nanoparticles from 10 to 30 nm containing small platinum particles (1 to 6 nm) on the surface. Flame-made Pt/Al_2O_3 shows slightly lower enantioselectivity, but much improved turnover frequencies in the hydrogenation of ethyl pyruvate compared to a conventionally used commercial standard hydrogenation catalyst. This improvement in activity is traced to the open and highly accessible structure of flame-made nanoparticle agglomerates, compared to the conventional porous catalysts.

Acknowledgments

We thank Professor D. Guenther (ETH) for the LA-ICP-MS and Dr. Frank Krumeich for the HRTEM measurements. Financial support by the Swiss National Science Foundation and the ETH is kindly acknowledged.

References

[1] G. Ertl, H. Knözinger, J. Weitkamp (Eds.), Handbook of Heterogeneous Catalysis, Vols. 1–5, VCH/Wiley, Weinheim, 1997.
[2] W.R. Moser, J.A. Knapton, C.C. Koslowski, J.R. Rozak, R.H. Vezis, Catal. Today 21 (1994) 157.
[3] T. Johannessen, S. Koutsopoulos, J. Catal. 205 (2002) 404.
[4] W.J. Stark, K. Wegner, S.E. Pratsinis, A. Baiker, J. Catal. 197 (2001) 182.

[5] W.J. Stark, S.E. Pratsinis, A. Baiker, J. Catal. 203 (2001) 516.
[6] K.L. Choy, H.K. Seh, Mater. Sci. Eng. A Struct. Mater. Prop. Microstruct. Process 281 (2000) 253.
[7] S.E. Pratsinis, Prog. Energy Combust. Sci. 24 (1998) 197.
[8] M.S. Wooldridge, Prog. Energy Combust. Sci. 24 (1998) 63.
[9] M. Sokolowski, A. Sokolowska, A. Michalski, B. Gokieli, J. Aerosol Sci. 8 (1977) 219.
[10] G.D. Ulrich, Chem. Eng. News 62 (1984) 22.
[11] Y. Orito, S. Imai, S. Niwa, Nguyen-gia-hung, J. Synth. Org. Chem. Jpn. 37 (1979) 173.
[12] Y. Orito, S. Imai, S. Niwa, Nippon Kagaku Kaishi 1118 (1979).
[13] Y. Orito, S. Imai, S. Niwa, Nippon Kagaku Kaishi 670 (1980).
[14] S. Niwa, S. Imai, Y. Orito, Nippon Kagaku Kaishi 137 (1982).
[15] A. Baiker, H.U. Blaser, in: G. Ertl, H. Knözinger, J. Weitkamp (Eds.), Handbook of Heterogeneous Catalysis, Vol. 5, Wiley/VCH, Weinheim, 1997, p. 2422.
[16] A. Baiker, J. Mol. Catal. A Chem. 115 (1997) 473.
[17] A. Baiker, J. Mol. Catal. A Chem. 163 (2000) 205.
[18] H.U. Blaser, H.P. Jalett, M. Muller, M. Studer, Catal. Today 37 (1997) 441.
[19] P.B. Wells, A.G. Wilkinson, Top. Catal. 5 (1998) 39.
[20] H.U. Blaser, H.P. Jalett, D.M. Monti, A. Baiker, J.T. Wehrli, Stud. Surf. Sci. Catal. 67 (1991) 147.
[21] K. Balázsik, B. Török, G. Szakonyi, M. Bartók, Appl. Catal. A Gen. 182 (1999) 53.
[22] W. Reschetilowski, U. Bohmer, J. Wiehl, Zeolites Relat. Micropor. Mater. State of the Art 1994 84 (1994) 2021.
[23] L. Mädler, H.K. Kammler, R. Mueller, S.E. Pratsinis, J. Aerosol Sci. 33 (2002) 369.
[24] L. Mädler, W.J. Stark, S.E. Pratsinis, J. Mater. Res. 17 (2002) 1356.
[25] S.R. Turns, An Introduction to Combustion: Concepts and Applications, McGraw–Hill, London, 1996.
[26] D. Günther, C.A. Heinrich, J. Anal. Atom. Spectrom. 14 (1999) 1363.
[27] J.H. Sinfelt, D.J.C. Yates, J.L. Carter, J. Catal. 24 (1972) 283.
[28] J.E. Benson, M. Boudart, J. Catal. 4 (1965) 704.
[29] H.U. Blaser, M. Garland, H.P. Jalett, J. Catal. 144 (1993) 569.
[30] R.M. Laine, T. Hinklin, G. Williams, S.C. Rand, in: Metastable, Mechanically Alloyed and Nanocrystalline Materials, Parts 1 and 2, Trans. Tech. Publications, Zurich-Uetikon, 2000, p. 500.
[31] Y.C. Xing, U.O. Koylu, D.E. Rosner, Combust. Flame 107 (1996) 85.
[32] G.M. Pajonk, Appl. Catal. 72 (1991) 217.
[33] S.J. Teichner, G.A. Nicolaon, M.A. Vicarini, G.E.E. Gardes, Adv. Colloid Interface Sci. 5 (1976) 245.
[34] Gmelin, Handbook of Chemistry 68 Pt., Chemie, Berlin, 1940, Main Vol.
[35] Y.F. Chu, E. Ruckenstein, J. Catal. 55 (1978) 281.
[36] G. Lietz, H. Lieske, H. Spindler, W. Hanke, J. Völter, J. Catal. 81 (1983) 17.
[37] H.U. Blaser, H.P. Jalett, D.M. Monti, J.F. Reber, J.T. Wehrli, Stud. Surf. Sci. Catal. 41 (1988) 153.
[38] G.A. Somorjai, G. Rupprechter, Stud. Surf. Sci. Catal. 109 (1997) 35.
[39] J.T. Wehrli, A. Baiker, D.M. Monti, H.U. Blaser, J. Mol. Catal. 49 (1989) 195.
[40] J.T. Wehrli, PhD thesis, 8833, ETH Zürich, 1989.
[41] T. Mallat, S. Frauchiger, P.J. Kooyman, M. Schurch, A. Baiker, Catal. Lett. 63 (1999) 121.
[42] G. Webb, P.B. Wells, Catal. Today 12 (1992) 319.
[43] G.A. Somorjai, M.A. Vanhove, Prog. Surf. Sci. 30 (1989) 201.